NJC

Reaction-induced macropore formation enabling commodity polymer derived carbons for CO2 capture

Journal:	*New Journal of Chemistry*
Manuscript ID	NJ-ART-11-2022-005434.R1
Article Type:	Paper
Date Submitted by the Author:	03-Dec-2022
Complete List of Authors:	Guillen Obando, Alejandro; The University of Southern Mississippi Robertson, Mark; University of Southern Mississippi, School of Polymer Science and Engineering Smith, Paul; University of Southern Mississippi, School of Polymer Science and Engineering Jha , Surabhi; University of Southern Mississippi Patton, Derek; University of Southern Mississippi, School of Polymers Qiang, Zhe; University of Southern Mississippi, School of Polymer Science and Engineering

Reaction-induced macropore formation enabling commodity polymer derived carbons for CO_2 capture

Alejandro Guillen Obando[1], Mark Robertson[1], Paul Smith[1], Surabhi Jha[1], Derek L. Patton[1], Zhe Qiang[1,]*

[1]School of Polymer Science and Engineering, The University of Southern Mississippi, 118 College Dr, Hattiesburg, MS, 39406

KEYWORDS: carbon capture, crosslinking, activation, pyrolysis, polyolefin

ABSTRACT

CO_2 capture from industrial point source waste streams represents an important need for achieving the global goal of carbon-neutrality. Compared with conventional liquid sorbents, solid sorbents can exhibit several distinct advantages, including enhanced lifetime and reduced energy consumption for sorbent regeneration. Considering CO_2 emission is a grand challenge, reaching

approximately 37 billion metric tons just in 2021, ideal sorbent solutions should not only exhibit high capture performance but also enable large scale manufacturing using low-cost precursors and simple processes. In this work, we demonstrate the use of a commodity polymer, polystyrene-*block*-polyisoprene-*block*-polystyrene (SIS), as the starting material for preparing hierarchically porous, sulfur-doped carbons for CO_2 capture. Particularly, sulfonation-crosslinking reaction enables the formation of macropores in the polymer framework due to the release of gaseous byproducts. After carbonization and activation, the highly porous structure of SIS-derived carbons is successfully retained, while their surface area can reach up to 905 m^2/g. These porous carbon sorbents exhibit excellent CO_2 uptake performance, reaching a sorption capacity of 3.8 mmol/g at 25 °C and 6.0 mmol/g at 0 °C, as well as a high selectivity up to 43:1 against N_2 gas at ambient conditions. Overall, our work provides an industrially viable method for "template-free" fabrication of porous carbons from commodity polyolefin-based materials, which can be employed for reducing CO_2 emission from industrial plants/sectors.

INTRODUCTION

Large-scale CO_2 emission into the atmosphere represents a major environmental concern due to its serious negative impacts on the climate and human health, including but not limited to global warming, air pollution, and respiratory diseases.[1–3] To address this challenge, significant

efforts have been employed for capturing emitted CO_2 gas from industrial point source waste streams (e.g., post-combustion capture),[4] primarily through developing sorbent-based technologies.[5,6] Particularly, a wide variety of solid sorbents with different materials chemistry, such as metal organic framework,[7] carbons,[8–10] polymers,[11,12] zeolites,[13,14] and silica,[15,16] have been developed for CO_2 capture, relying on chemical and/or physical adsorption mechanisms. Compared with their conventional liquid counterparts, solid sorbents in general can exhibit improved thermal stability, while providing several potential advantages such as the ability of long-term CO_2 storage and lower energy penalty for subsequent CO_2 release.[17] Porous carbons, as a class of the most promising material solutions, are especially attractive due to their high chemical and thermal stability, relatively low-cost, and broad compatibility with additional surface chemistry to further enhance CO_2 capture performance.[18]

A variety of functionalization methods have been investigated as potential routes to improve the performance of carbon sorbents for CO_2 capture, such as activation,[19,20] and heteroatom doping,[21,22] Chemical activation of carbons is an industrially relevant approach (low-cost and easy to scale up), which can be accomplished through using chemical agents to selectively react with carbon and remove portions of the framework. The activation process leads to the

formation of micropores, thus increasing surface area of carbons and allowing for more sorption sites. Wickramaratne et al. prepared activated carbon particles with diameters in the range of 200 nm and 400 nm, and high surface areas up to 2400 m^2/g using CO_2 gas to activate phenolic resin-derived carbons. These materials exhibited a CO_2 adsorption capacity of 4.55 mmol/g at room temperature.[23] Moreover, the presence of heteroatoms in the carbon framework can enable favored interactions between carbon surface and CO_2 molecules.[24] As an example, Shi et al. prepared nitrogen and sulfur co-doped, hierarchically porous carbons through combining chemical doping and activation, which resulted in a CO_2 uptake capacity of up to 2.4 mmol/g at 1 bar.[25] Inclusion of nitrogen heteroatoms into mesoporous carbons, through using dicyandiamide as the dopant, can result in a CO_2 adsorption capacity of 3.2 mmol/g at room temperature.[26] Notably, various dopants can be used to fabricate porous carbons with controlled heteroatom content.[27–31] Alternatively, a simple method to prepare nitrogen-doped carbons is through direct pyrolysis of heteroatom-containing polymeric precursors or biomass,[32] including polyacrylonitrile,[33] commercial urea-formaldehyde resin,[34] mesitylene,[35] and waster chestnut shell;[36] their derived carbons can exhibit a relatively high CO_2 uptake performance, which are in the range of 3.5 mmol/g – 7 mmol/g at 1 bar. In general, both chemical activation and heteroatom doping are viable methods to enhance

CO_2 uptake, enabled by the presence of micropores for increasing sorption sites, and the improved affinity of CO_2 molecules to the carbon framework.

The gas uptake capacity of porous carbon is primarily determined by their porosity, micropore volume, and surface area (e.g., Dubinin theory), while the presence of macro- and meso-pores can enhance the sorbate diffusion kinetics.[37–41] Informed by this material design concept, many studies have focused on developing CO_2 capture sorbents containing pores at different length scales, from nano to macro. In general, conventional methods to create macropores include using templating agents, solvent exchange, and foaming agents. Specifically, colloids,[42] nanoparticles,[43] and polymers[44,45] can be employed to generate pores with controlled structures, but typically have low product yields with respect to the total consumption of raw materials required for synthesis. While these established methods for developing macropores are effective, designing a process which inherently produces macropores would be advantageous by reducing process complexity and cost.[46,47] Particularly, template-free methods for fabricating porous carbons can enable a streamlined process for materials preparation, providing high potential toward scale-up production and commercialization.[48,49]

Previous studies demonstrate the use of polyolefin homopolymers as carbon precursors, with common examples of carbon fiber production and plastic waste upcycling.[50–54] Our group recently reported an approach for upcycling waste polypropylene masks to sulfur-doped carbon fibers as a viable material solution for CO_2 capture.[55] However, this method requires the polymer precursors having pre-existing fibril structures, which is critical for efficient crosslinking and CO_2 uptake. The ability to convert bulk polyolefin-based polymers to porous carbons remains largely underexplored. Herein, we demonstrate a simple method to synthesize hierarchically porous carbon sorbents by using polystyrene-*block*-polyisoprene-*block*-polystyrene (SIS) as the precursor and sulfonation-based chemistry for crosslinking. SIS is a common type of low-cost commodity thermoplastic elastomer, which is widely used in various applications.[56] During crosslinking, it was found that SIS can have much faster reaction kinetics than semi-crystalline polyolefins, while the gaseous by-products can enable macropore formation within the framework. After carbonization and chemical activation steps, SIS-derived carbon materials can exhibit a high CO_2 adsorption capacity of 3.8 mmol/g at room temperature and 6.0 mmol/g at 0 °C and 1 bar. The combined use of low-cost commodity plastics and a simple process for preparing hierarchical

porous carbons renders our system to be a potential industrially viable approach for scaled production of solid CO_2 capture sorbents.

EXPERIMENTAL SECTION

Materials

Sulfuric acid (98 wt%) and potassium hydroxide (KOH) were purchased from Thermo Fisher. Polystyrene-*block*-polyisoprene-*block*-polystyrene (SIS) (14 vol% of styrene content, molecular weight: 102,500 g/mol, Đ: 1.12) was obtained from Sigma Aldrich. Deionized (DI) water was obtained using a Milli-Q IQ 7003 ultrapure lab water purification system.

SIS crosslinking, carbonization, and activation

SIS pellets were first weighed out (1.2 g) and placed in a 50 mL glass beaker, where 25 mL of 98% sulfuric acid was introduced. These materials were then heated at 140 ˚C using a Thermolyne electric muffle furnace. After reaction, samples were carefully collected from the beaker and washed with DI water for three times. Subsequently, crosslinked SIS was completely

dried at elevated temperatures (140 ˚C) under vacuum, and then carbonized in a tube furnace (MTI Corporation OTF-1200x) using a heating ramp of 1 °C/min to 600 ˚C, and 5 ˚C/min to 800 ˚C under N_2 atmosphere. For SIS samples crosslinked at different temperatures, a similar procedure was used while the crosslinking time was varied. Activation was performed utilizing carbonized SIS and KOH blend, which was then reacted at 700 ˚C under nitrogen atmosphere. Specifically, a 1:1 mass ratio of SIS and KOH blend was activated for 30 min, 60 min, and 90 min, respectively. 1: 0.5 and 1: 2 mass ratios of SIS-derived carbon to KOH were also employed, which were activated for 60 min. After KOH activation, these samples were washed three times in centrifuge tubes using 45 mL of DI water and dried at 100 ˚C in a vacuum oven to obtain carbon powder.

Characterization methods

Changes in the chemical composition of SIS during crosslinking were determined using a PerkinElmer Frontier attenuated total reflection Fourier transform infrared (FTIR) spectrometer, with a scan range of 4000−600 cm^{-1} running over 32 scans in average at a resolution of 4 cm^{-1}. Micrographs of SIS samples after crosslinking, carbonization and activation were obtained using a Zeiss Ultra 60 field-emission scanning electron microscope (SEM). Macropore diameters were measured using ImageJ software. A Micromeritics Tristar II instrument was used to determine

pore textures of SIS-derived carbons, including their adsorption and desorption isotherms under N_2 at 77 K. Surface area was determined using Brunauer-Emmett-Teller (BET) analysis, while the pore size distribution was calculated using the non-local density functional theory (NLDFT) model. Additionally, this instrument was employed to obtain CO_2 and N_2 sorption performance of carbons at ambient temperature by measuring their respective adsorption-desorption isotherms from 0.01 to 1 bar. X-ray photoelectron spectroscopy (XPS) was performed on a Thermo Fisher ESCALAB Xi+ spectrometer equipped with a monochromatic Al X-ray source (1486.6 eV) and a MAGCIS Ar+/Ar_n+ gas cluster ion sputter gun. Measurements were performed using the standard magnetic lens mode and charge compensation. The base pressure in the analysis chamber during spectral acquisition was at 3×10^{-7} mbar. Binding energies were calibrated with respect to the C1s peak at 284.8 eV. Thermo Scientific Avantage analysis software v5.9904 was used to analyze heteroatom content of SIS-derived carbon samples. SAXS experiments were conducted on a laboratory beamline system (Xenocs Inc. Xeuss 2.0) with an X-ray wavelength of 1.54 Å and sample to detector distance of 4 m. Samples were kept under vacuum to minimize air scattering. SAXS data reduction and analysis were performed using Nika software. Thermogravimetric analysis (TGA) was conducted using a Discovery Series TGA 550 (TA Instruments) to determine

char yield of polymer precursors, as well as characterize the sorption behaviors of carbon sorbents with a continuous CO_2 flow at 30 ml/min.

RESULTS AND DISCUSSION

SIS crosslinking is enabled by a sulfonation-based chemical reaction, which is similar to previously described approaches for polyolefin materials.[57,58] During this step, both polyisoprene (PI) and polystyrene (PS) segments can be functionalized with sulfonic acid groups. The crosslinking reaction of SIS is shown in Figure 1(A), which includes multiple reaction mechanisms that occur concurrently. For polyethylene and polypropylene, the initial step in the crosslinking process is the addition of sulfonic acid functional groups to the polymer backbone, followed by elimination to form double bonds. These double bonds can then be initiated to participate in crosslinking. A similar reaction mechanism is anticipated for the PI block in SIS, while the presence of double bonds in the polymer backbone may result in enhanced reaction kinetics. Additionally, sulfonation of PS using sulfuric acid is an established process, which can achieve nearly 100% degree of functionalization.[59] As shown in Figure 1(B), the mass of SIS increases

with extending reaction time, reaching a plateau value of approximately 50 wt% after 1 h. This result indicates that the crosslinking reaction kinetics of SIS is significantly faster than that of polyolefin homopolymers in the literature, especially considering the SIS employed in this study were in pellet form, with an averaged diameter of 2-3 mm. We attributed the enhanced kinetics to the amorphous nature of PI matrix (Figure S1), which significantly accelerated the acid diffusion within the polyolefins due to the absence of crystallinity. Figure 1(C) shows the FTIR spectra of SIS as a function of crosslinking time. Specifically, the stretching vibrations at 1127 cm^{-1} is associated with the presence of sulfonic acids installed on the polymer backbone, which can be observed after crosslinking for 40 min. The band at 1032 cm^{-1} is representative of the sulfonation of the aromatic rings within the PS block of the polymer, which can undergo nearly quantitative sulfonation degree in sulfuric acid within 1 h at elevated temperatures.[59] The PS sulfonation occurs simultaneously with the crosslinking of the PI block. As the reaction progresses, the intensity of bands at 1644 cm^{-1} increases, which corresponds to the formation of C=C stretching in polymers. This result suggests that while the alkenes inherent to the PI segments can undergo radical initiation to form crosslinks, further additions, eliminations, and rearrangements also occurred along the polymer chains to form crosslinked sites. The band representing C-H bond stretching

was found at 2918 cm^{-1} in the initial SIS sample and decreased in intensity after 40 min and completely disappeared after 90 min. Hydroxyl groups in the polymer system were also formed through the sulfonation reaction, as indicated by the formation of a broad peak at 3362 cm^{-1}. The FTIR spectra of crosslinked SIS remains nearly constant after extending crosslinking time above 90 min (Figure S2). Therefore, utilizing SIS as the carbon precursor, we can successfully address the previous challenge of diffusion-limited crosslinking of polyolefin materials, which is a key bottleneck in scaled manufacturing of their derived carbon materials.

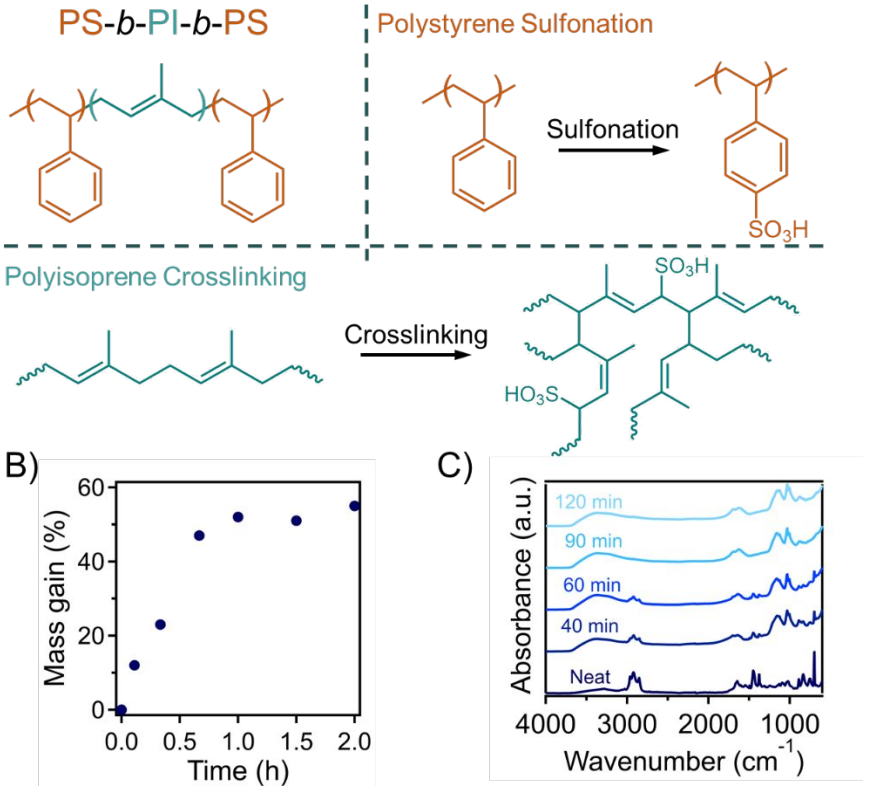

Figure 1. (A) A simplified reaction scheme showing the sulfonation-enabled crosslinking SIS. (B) Mass gain and (C) FTIR spectra of crosslinked SIS as a function of crosslinking time at 140 °C.

Upon crosslinking, it was found that macropores were generated within the SIS materials, which can be attributed to the gaseous by-products released from the polymer matrix.[60,61] Figure 2(A) shows the SEM micrograph of a pristine SIS sample, which has a smooth and uniform surface at a macroscopic scale. After sulfonating at 140 ˚C for 40 min, macropores were observed in the polymer framework (Figure 2(B)), which further developed upon extending the reaction time. Figure 2(C-D) shows the SEM images of crosslinked SIS samples after 60 min and 90 min reaction time, which are highly porous and have a majority of pores with diameters ranging from 4.3 μm to 6.0 μm. The macropore formation in this process is driven by the rigorous reaction of the PI segment crosslinked using concentrated sulfuric acid at 140 °C. The release of gaseous byproducts, primarily SO_2 and CO_2, can disrupt the rubbery SIS framework, and thus form macropores. Notably, our approach can produce relatively uniform pores through a template-free method, which is easy to scale-up.

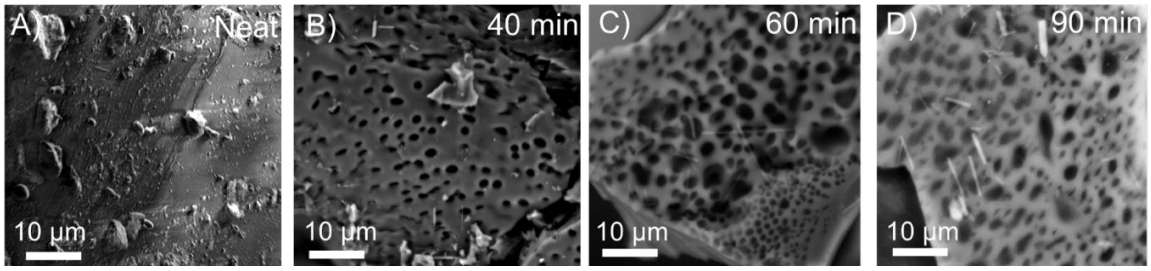

Figure 2. SEM images of A) pristine SIS and SIS crosslinked within concentrated sulfuric acid at 140 °C for B) 40 min, C) 60 min, D) 90 min.

To further elucidate how the crosslinking reaction conditions impact the development of macropores within SIS, two different crosslinking temperatures were employed, including 70 ˚C and 100 ˚C. Both temperatures result in fully crosslinked SIS, while different times were required (24 h for 70 ˚C and 2 h for 100 ˚C) as evidenced by the mass uptake and FTIR results (Figure S3 and S4). Previous reports indicate that at least 90 ˚C is needed for the crosslinking of polyethylene and polypropylene to occur within the sulfuric acid, while we found that PI requires milder reaction conditions for reaching a fully crosslinked state. As shown in Figure 3(A-B), both crosslinked SIS samples (70 ˚C for 24 h and 100 ˚C for 2 h) contain macropores, with similar averaged sizes as samples shown in Figure 2(C-D). These results further indicate that our approach of reaction-induced pore formation is applicable for a wide range of processing conditions, enabling their potential broad use for preparing macroporous polymer materials. Furthermore, SAXS was

employed to characterize the nanostructure of SIS after crosslinking reactions. As shown in Figure S5(A), the neat SIS sample has multiple ordering peaks, suggesting the presence of ordered cylindrical structures due to spontaneous microphase separation between distinct segments. The primary ordering peak was at 0.201 nm^{-1}, corresponding to a domain spacing of 31.3 nm. However, fully crosslinking SIS samples (including three different crosslinking temperatures) leads to the complete disappearance of ordering peaks in the SAXS patterns, indicating the disordered structures, as shown in Figure S5(B). The loss of ordering can be attributed to the sulfonation reaction employed in the crosslinking process. In some seminal works, the reaction induced disordering of block copolymers was also observed. Specifically, *in-situ* polymer grafting onto poly(styrene)-*block*-poly(butadiene) can lead to nanostructural transition with a decreased degree of ordering.[62] Similarly, in-film photopolymerization of monomer vapors within SIS films can disrupt the pre-ordered nanostructures.[63,64] The sulfonation of PI and PS blocks in our systems may lead to increased miscibility between distinct domains due to their reduced Flory-Huggins interaction parameter, while the macropore formation process can also largely disrupts the ordered nanostructures. These phenomena collectively lead to a completely disordered morphology of SIS samples after fully crosslinked by sulfonation chemistry.

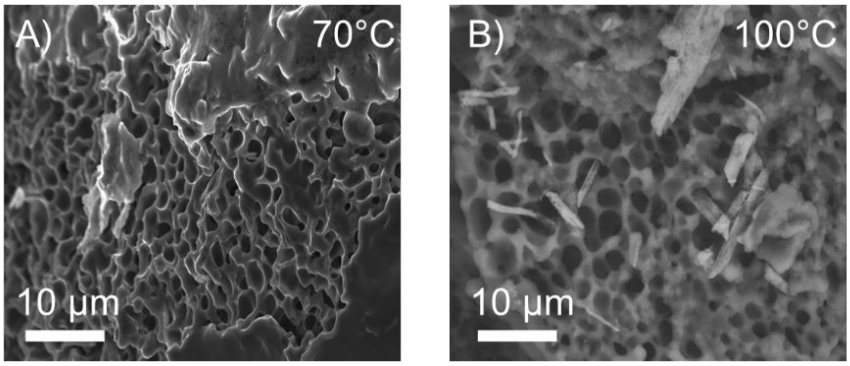

Figure 3. SEM images of crosslinked SIS samples, which were reacted at A) 70 °C for 24 h, and B) 100 °C for 2 h.

Crosslinked SIS was then pyrolyzed at 800 ˚C under an inert atmosphere, with a product yield of approximately 35 wt%. As shown in Figure S6, pristine SIS is completely decomposed at temperatures beyond 435 °C under nitrogen atmosphere. Upon carbonization, the crosslinked polyolefin matrix in SIS was converted to carbon materials, while PS segments were thermally decomposed. Figure 4(A) shows the morphology of carbonized SIS samples (crosslinked at 140 ˚C for 90 min), indicating that the macropores can be successfully retained, with similar pore diameters in the range of 4.4 µm-6.3 µm as compared to the crosslinked samples. Additionally, the nitrogen physisorption isotherm of carbonized SIS in Figure S7 (pore size distribution is included in Figure S8) indicates a low BET surface area of 37 m^2/g. In addition to the presence of macropores, the SIS-derived carbon material presents another important feature, which is the

inclusion of sulfur heteroatoms within the framework. The presence of sulfur and oxygen is confirmed by the XPS spectrum shown in Figure 4(B, C) and Figure S9, in which the doping content of sulfur heteroatoms within the SIS-derived carbon is approximately 2 at%. This result is slightly lower compared to our recent study of upcycling mask waste to multifunctional carbon fibers.[55] We attribute this difference to much longer reaction times in our previous study which extended up to 12 h. When comparing shorter reaction times in the polypropylene fiber-based system, the doping contents are comparable (1.9 at% for 90 min in this study compared to 2.3 at% for 2 h in the previous study).[55] Sulfur doping can lead to enhanced CO_2 sorption as shown in the literature,[65] and the type of sulfur moiety within the carbon framework also plays a significant role. Here, we found that 72.5 at% of sulfur heteroatom is in the form of C-S-O (Figure 4(C)), derived from the sulfonate functional groups, which is the most favorable type to strengthen molecular-level interactions between carbon surface and CO_2 molecules.

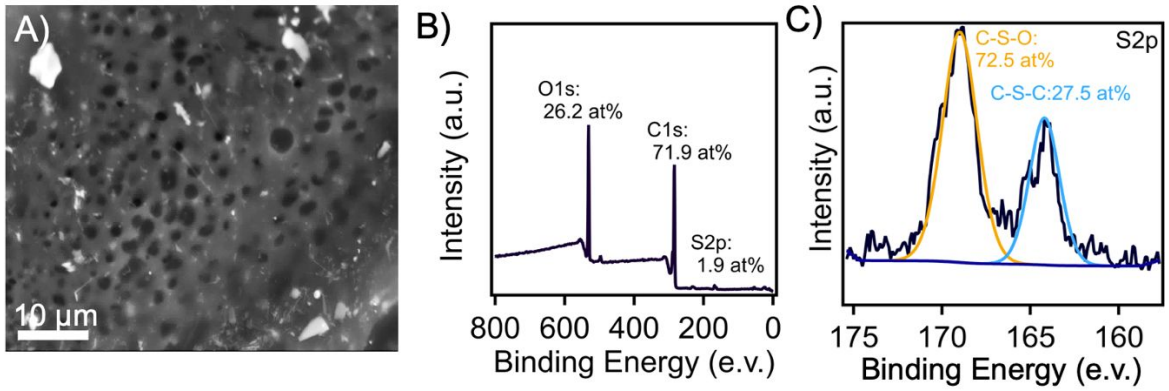

Figure 4. A) SEM image of carbonized SIS samples, showing retention of pores formed during crosslinking reaction. B) XPS spectrum of carbonized SIS, including the atomic percentage of O 1s, C 1s, and S 2p. C) High resolution XPS scan of S 2p

Figure 5 shows the CO_2 sorption performance of three different SIS-derived porous carbons, which were fully crosslinked at different temperatures. These materials exhibited very similar adsorption capacity of CO_2 molecules at room temperature (25 °C) and 1 bar, which are 2.0 mmol/g, 2.0 mmol/g, and 2.1 mmol/g, corresponding to samples crosslinked at 70 °C, 100 °C, and 140 °C, respectively. While these materials exhibit very similar low surface areas (Figure S10), their CO_2 uptake performance is comparable with many other reported porous carbons with significantly higher surface areas. For example, nitrogen-doped hollow carbon nanospheres, with a surface area of 767 m^2/g, exhibit a CO2 uptake capacity of approximately 2.5 mmol/g at room temperature and 1 bar.[66] Similarly, templated porous carbons with surface areas in the range from

800 m^2/g to 1400 m^2/g can uptake 2-2.5 mmol/g of CO2 at 25 °C and 1 bar.[67] These results further confirm that sulfur heteroatom in the carbon framework can effectively alter the electro-negativity of porous carbon surface, enabling enhanced interactions between sorbent and sorbates (CO_2 molecules).[68,69] Additionally, The consistent performance from different SIS-derived carbon sorbents further confirms that the key role of microporosity in determining CO_2 capture sorption. These values were slightly lower than our previous report of sulfur-doped carbon fibers derived from mask waste, which exhibited a CO_2 uptake capacity of 3.1 mmol/g under identical CO_2 sorption conditions.[55] We believe this difference is associated with the surface area of our SIS-derived carbons, since the carbon fiber recorded a BET surface area up to 361 m^2/g. However, the requirement of pre-existing fibril structures within mask waste may limit its broad adoption. Furthermore, previous results indicate that polyolefin crosslinking using sulfuric acid is a diffusion-limited process. Herein, through utilizing the highly reactive and amorphous PI phases in the precursors, this method provides much faster reaction kinetics, an inherent pore formation mechanism, and can be applied to a broad range of SIS-based materials without any previous treatment required for creating pre-defined structures.

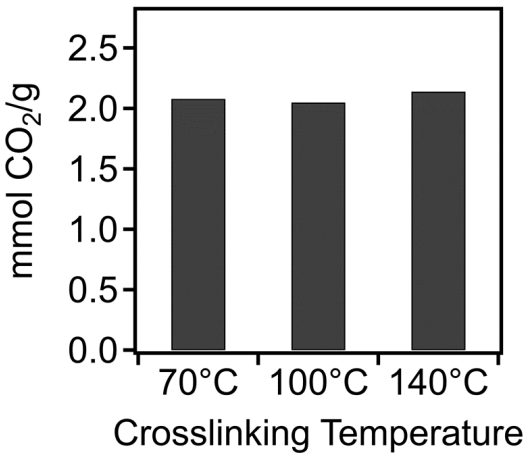

Figure 5. CO_2 adsorption isotherm of different carbonized SIS samples, which were fully crosslinked at 70 °C for 24 h, 100 °C for 2 h, and 140 °C for 90 min.

As discussed earlier, there are several efficient routes for functionalizing SIS-derived carbon materials to enhance their CO_2 adsorption capacity. Considering the low surface area is a performance-limiting factor in our systems, chemical activation of these carbon materials was employed using KOH. To briefly describe this process, KOH can react with carbons at high temperatures (> 500 °C) for partial framework etching/removal, while the KOH/carbon ratio can dictate the micropore formation mechanisms.[70] In this work, a KOH/carbon mass ratio of 1:1 was employed to allow the generation of micropores with an interconnected morphology.[71] Porous carbon derived from SIS crosslinked at 140 °C for 90 min was employed for activation process.

Figure 6(A) shows the liquid nitrogen sorption isotherms of activated SIS-derived carbons, of which surface areas increased from 767 m^2/g to 796 m^2/g and 905 m^2/g by extending the activation time from 30 min to 60 min and 90 min (activation was performed at 700 °C under N_2). The introduction of micropores through activation was confirmed by their characteristic type I isotherm, which corresponds to the presence of both micropores and macropores. Figures S11 displays the pore size distribution of these samples upon applying different chemical activation times, which all demonstrated a significant increase in the micropore volume compared to their counterpart prior to activation. Other KOH to carbon mass ratios were also employed for the activation process in order to control the surface area of resulting carbons. Figure S12 shows the sorption isotherms of activated carbons using both 1:0.5 and 1:2 mass ratios of SIS-derived carbon and KOH, which has a surface area 256 m^2/g and 707 m^2/g, respectively. SEM imaging confirmed that the macropores formed during the SIS crosslinking step were retained after our KOH activation process, as shown in Figure 6 (B). The average diameters of these macropores were still in the range of 4-6 μm, which is similar to the carbonized samples. Furthermore, after activation (KOH to carbon mass ratio is 1:1), the sulfur content decreased with prolonged reaction times. The amount of oxygen in the samples initially increased to 33.4 at% but decreased to 16.8 at% after 90

minutes of reaction. Specifically, both O-C-O and C-S-O bonds are retained from the SIS-derived carbon prior to activation, while C-S-C bonds are no longer present, as shown in Figure S13. As demonstrated in a previous study, the presence of sulfoxide bonds within the carbon framework can be instrumental in optimizing the materials CO_2 uptake capacity.[55]

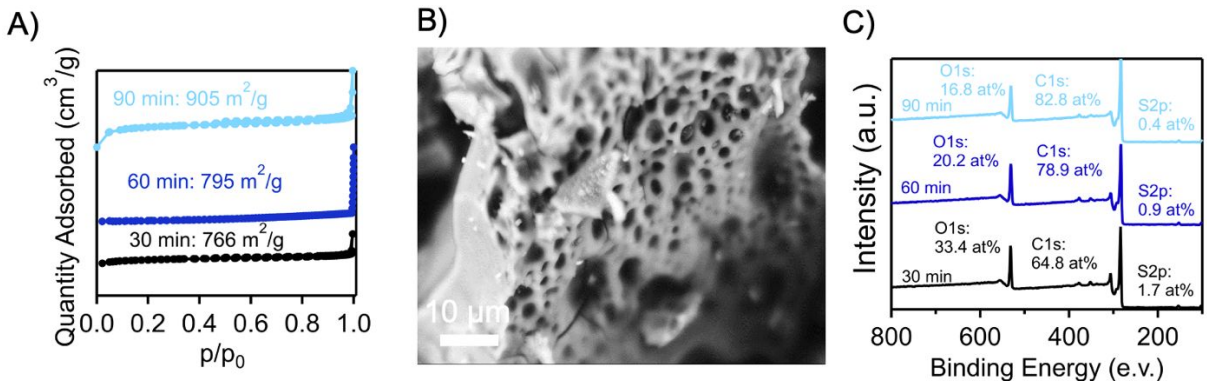

Figure 6. A) Adsorption-desorption isotherm, B) SEM image demonstrating pore retention, and C) XPS survey scam spectra of SIS-derived carbons after different activation time.

The CO_2 adsorption capacity of activated SIS-derived carbons at ambient temperature are shown in Figure 7(A). Upon activation for 30 min, the CO_2 uptake of these porous carbons changed from 2.1 mmol/g to 3.5 mmol/g, corresponding to a more than 65% increase through the creation of micropores. Further extending the activation time to 60 min and 90 min leads to a CO_2 sorption capacity of 3.7 mmol/g and 3.8 mmol/g which corresponds well with their increased surface areas.

This result indicates the role of micropores for determine CO_2 capture performance of porous carbons, despite a slight decrease in sulfur doping content after the activation step. Notably, at 0.15 bar, a condition which is relevant to CO_2 concentrations in flue gases, these materials show a relatively high CO_2 uptake ranging from 1.18-1.21 mmol/g. Furthermore, these materials exhibit a higher CO_2 uptake of 5.4 mmol/g, 5.3 mmol/g, and 6.0 mmol/g at 0 °C, corresponding to the samples activated for 30 min, 60 min, and 90 min, respectively. These results confirm that the presence of hierarchical pores within activated SIS-derived carbons can lead to excellent CO_2 capture performance, which is comparable or higher than several recent reports.[72,73] For example, a very recent work from Mohamed et al. reported the development of porous organic polymers linked with crown ether and benzoxazine through a multi-step procedure, which can uptake CO_2 up to 5.8 mmol/g at 0 °C.[74] Moreover, using the CO_2 sorption capacity of activated SIS-derived carbons at 0 °C and 25 °C and various pressure, heat of adsorption for these samples can be determined according to Clausius-Clapeyron equation, which is in the range of 15-28 kJ/mol, consistent with physisorption mechanism and suggesting small amount of energy would be enough for sorbent regeneration. Furthermore, gas sorption selectivity measurements of these samples were performed to compare their performance between two different gas molecules, including CO_2

and N_2, which are very common in post-combustion flue gases. As shown in Figure 7(B), these SIS-derived activated carbons showcase a high selectivity for CO_2 over N_2 of 69:1 at 0 °C and 43:1 at 25 °C, which is important for application relevant conditions. For comparison, activated carbons prepared from cellulose and chitosan char typically exhibit an CO_2/N_2 selectivity of 42:1 and 37:1, respectively. [75, 76] For other activated carbon samples, they exhibit slightly lower sorption performance as shown in Figure S14, which can be attributed to their lower surface area. Notably, our method only requires low-cost commodity thermoplastic elastomers as the precursors, along with simple, scalable processes for the generation of bimodal pores, enabling the high potential toward scaled production.

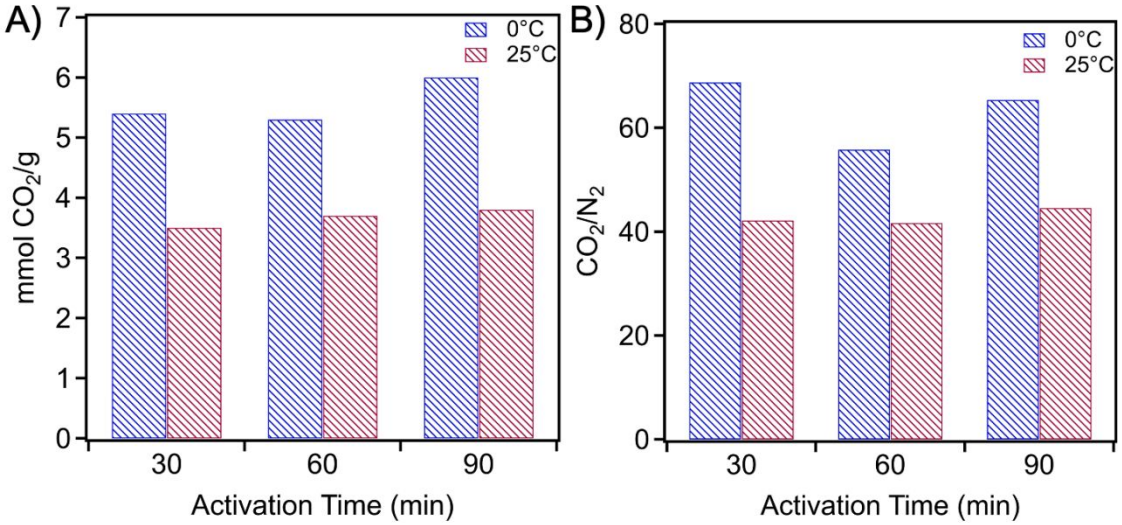

Figure 7. (A) CO_2 adsorption capacity and (B) CO_2/N_2 selectivity of activated SIS-derived at 0 °C and 25 °C. KOH activation was performed at 700 °C. The mass ratio of SIS-derived carbon to KOH is 1:1.

Finally, we examine the cycle stability of SIS derived, hierarchically porous carbon for CO_2 capture and release, which is important for informing their long-term use and performance. As shown in Figure S15(A), under saturated CO_2 environment, the carbon sorbents can increase approximately 14% of its original weight attributed to the sorption of CO_2 molecules, which is consistent with their uptake capacity determined by physisorption measurements. By heating the materials to 130 ºC, a complete mass recovery was observed, suggesting a full release of CO_2 upon desorption through thermal treatment. Furthermore, the sorbent exhibits an excellent cycle stability, retaining over 94% of CO_2 sorption capacity after 40 cycles (Figure S15(B)), which confirms the highly reversible interactions between carbon framework and CO_2 gases through adsorption mechanisms. The excellent recyclability further strengthens the potential of these porous carbons, which are converted from commodity polymer using a simple process, for efficiently capturing CO_2 with durable performance and sustainable use.

CONCLUSIONS

In this study, sulfur doped, hierarchically porous carbons were prepared through steps of crosslinking, carbonization, and activation, using commodity SIS as the precursor. The crosslinking reaction, accomplished by heating SIS samples in concentrated sulfuric acid at

elevated temperatures, leads to the macropore formation in polymer framework due to the release of gaseous by-products. With varying crosslinking time and temperature, this approach results in similar pore textures of crosslinked SIS, suggesting its broad applicability and insensitivity to processing conditions. Upon pyrolysis under nitrogen atmosphere, SIS-derived macroporous carbons demonstrate a CO_2 uptake capacity up to 2.1 mmol/g at 25 °C and 1 bar. Further activating these carbons using KOH leads to significantly improved surface area from ~38 m^2/g to as high as 905 m^2/g, which enables an excellent CO_2 adsorption capacity of 6.0 mmol/g at 0 °C and 3.8 mmol/g at 25 °C. Our system has advantages of using low-cost polymer precursors and simple manufacturing processes, which can provide a feasible material solution for combating CO_2 emission from industrial sectors. Moreover, the ability to create macropores through sulfonation-based crosslinking reactions of polyolefins can be extended to other systems for fabricating porous materials for broad applications.

ASSOCIATED CONTENT

Supporting Information.

Supporting information includes following data: Differential scanning calorimetry thermogram for a pristine SIS bead, mass gain and FTIR spectra of samples crosslinked at 70 °C and 100 °C, TGA analysis of pristine SIS, BET adsorption-desorption isotherm of carbonized SIS, high-resolution XPS spectra for carbonized SIS and after activation at different periods of time, pore textures (surface areas, pore area) for carbonized materials, and CO_2 adsorption cycle stability.

This material is available free of charge.

AUTHOR INFORMATION

Corresponding Author

Zhe Qiang, Email: zhe.qiang@usm.edu

Author Contributions

The manuscript was written through contributions of all authors. All authors have given approval to the final version of the manuscript.

Funding Sources

This work was partially supported by the Mississippi SMART Business Act. The purchase of the XPS instrumentation used in this work was supported by the NSF Major Research Instrumentation program (DMR-1726901). Z.Q. would like to thank financial support from the University of Southern Mississippi.

ACKNOWLEDGMENT

The authors would like to acknowledge Dr. Xiaodan Gu and Guorong Ma for assisting with SAXS experiments.

REFERENCES

1 K. O. Yoro and M. O. Daramola, CO2 Emission Sources, Greenhouse Gases, and the Global Warming Effect, *Advances in Carbon Capture*, 2020, 3–28.

2 G. D'Amato, H. J. Chong-Neto, O. P. Monge Ortega, C. Vitale, I. Ansotegui, N. Rosario, T. Haahtela, C. Galan, R. Pawankar, M. Murrieta-Aguttes, L. Cecchi, C. Bergmann, E. Ridolo, G. Ramon, S. Gonzalez Diaz, M. D'Amato and I. Annesi-Maesano, The Effects of Climate Change on Respiratory Allergy and Asthma Induced by Pollen and Mold Allergens, *Allergy*, 2020, **75**, 2219–2228.

3 N. mac Dowell, P. S. Fennell, N. Shah and G. C. Maitland. The Role of CO2 Capture and Utilization in Mitigating Climate Change, *Nat. Clim. Change 2017 7:4*, 2017, **7**, 243–249.

4 P.C. Psarras, S. Comello, P. Bains, P. Charoensawadpong, S. Reichelstein, J. Wilcox. Carbon Capture and Utilization in the Industrial Sector, *Environ. Sci. Technol*. 2017, **51**, 19, 11440-11449.

5 H. A. Patel, J. Byun and C. T. Yavuz, Carbon Dioxide Capture Adsorbents: Chemistry and Methods, *ChemSusChem*, 2017, **10**, 1303–1317.

6 W. Gao, S. Liang, R. Wang, Q. Jiang, Y. Zhang, Q. Zheng, B. Xie, C. Y. Toe, X. Zhu, J. Wang, L. Huang, Y. Gao, Z. Wang, C. Jo, Q. Wang, L. Wang, Y. Liu, B. Louis, J. Scott, A.

C. Roger, R. Amal, H. He and S. E. Park, Industrial Carbon Dioxide Capture and Utilization: State of the Art and Future Challenges, *Chem. Soc. Rev.*, 2020, **49**, 8584–8686.

7 J. bin Lin, T. T. T. Nguyen, R. Vaidhyanathan, J. Burner, J. M. Taylor, H. Durekova, F. Akhtar, R. K. Mah, O. Ghaffari-Nik, S. Marx, N. Fylstra, S. S. Iremonger, K. W. Dawson, P. Sarkar, P. Hovington, A. Rajendran, T. K. Woo and G. K. H. Shimizu, A Scalable Metal-Organic Framework as a Durable Physisorbent for Carbon Dioxide Capture. *Science*, 2021, **374**, 1464–1469.

8 J. Wang, L. Huang, R. Yang, Z. Zhang, J. Wu, Y. Gao, Q. Wang, D. O'Hare and Z. Zhong, Recent Advances in Solid Sorbents for CO2 Capture and New Development Trends, *Energy Environ. Sci.*, 2014, **7**, 3478–3518.

9 P. Staciwa, U. Narkiewicz, D. Sibera, D. Moszyński, R. J. Wróbel and R. D. Cormia, Carbon Spheres as CO2 Sorbents, *Appl. Sci.* , DOI:10.3390/APP9163349.

10 Q. F. Deng, L. Liu, X. Z. Lin, G. Du, Y. Liu and Z. Y. Yuan, Synthesis and CO2 Capture Properties of Mesoporous Carbon Nitride Materials*, Chem. Eng. J.*, 2012, **203**, 63–70.

11 A. P. Hallenbeck and J. R. Kitchin, Effects of O2 and SO2 on the Capture Capacity of a Primary-Amine Based Polymeric CO2 Sorbent. *Ind. Eng. Chem. Res.*, 2013, **52**, 10788–10794.

12 A. Y. Tsivadze, O. E. Aksyutin and A. G. Ishkov, A Review on Polymer Based Adsorbents for CO2 Capture., *IOP Conf. Ser. Mater. Sci. Eng.*, 2021, **1114**, 012081.

13 F. Su, C. Lu, S. C. Kuo and W. Zeng, Adsorption of CO2 on Amine-Functionalized y-Type Zeolites., *Energy Fuels*, 2010, **24**, 1441–1448.

14 Q. Wang, W. Xia, W. Guo, L. An, D. Xia and R. Zou, Functional Zeolitic-Imidazolate-Framework-Templated Porous Carbon Materials for CO2 Capture and Enhanced Capacitors. *Chem. Asian. J.*, 2013, **8**, 1879–1885.

15 M. Niu, H. Yang, X. Zhang, Y. Wang and A. Tang, Amine-Impregnated Mesoporous Silica Nanotube as an Emerging Nanocomposite for CO2 Capture, *ACS Appl. Mater. Interfaces*, 2016, **8**, 17312–17320.

16 J. J. Lee, C. Sievers and C. W. Jones, Silica-Supported Hindered Aminopolymers for CO2 Capture., *Ind. Eng. Chem. Res.*, 2019, **58**, 22551–22560.

17 Z. Zhang, T. Wang, M. J. Blunt, E. J. Anthony, A. H. A. Park, R. W. Hughes, P. A. Webley and J. Yan, Advances in Carbon Capture, Utilization and Storage., *Appl. Energy*, 2020, **278**, 115627.

18 A. E. Creamer and B. Gao, CO2 Capture: A Critical Review., *Environ. Sci. Technol.*, 2016, **50**, 7276–7289.

19 N. Abuelnoor, A. AlHajaj, M. Khaleel, L. F. Vega and M. R. M. Abu-Zahra, Activated carbons from biomass-based sources for CO2 capture applications, *Chemosphere*, 2021, **282**, 131111.

20 J. Sreńscek-Nazzal and K. Kiełbasa,_Advances in modification of commercial activated carbon for enhancement of CO2 capture, *Appl. Surf. Sci.*, 2019, **494**, 137–151.

21 Y. Wang, M. Wang, Z. Wang, S. Wang and J. Fu,_Tunable-quaternary (N, S, O, P)-doped porous carbon microspheres with ultramicropores for CO2 capture, *Appl. Surf. Sci.*, 2020, **507**, 145130.

22 D. Li, Y. Chen, M. Zheng, H. Zhao, Y. Zhao and Z. Sun, Hierarchically Structured Porous Nitrogen-Doped Carbon for Highly Selective CO2 Capture, *ACS Sustain. Chem. Eng.*, 2016, **4**, 298–304.

23 N. P. Wickramaratne and M. Jaroniec, Activated carbon spheres for CO2 adsorption, *ACS Appl. Mater. Interfaces*, 2013, **5**, 1849–1855.

24 M. Seredych, J. Jagiello and T. J. Bandosz, Complexity of CO2 adsorption on nanoporous sulfur-doped carbons – Is surface chemistry an important factor? *Carbon*, 2014, **74**, 207–217.

25 J. Shi, H. Cui, J. Xu, N. Yan, C. Zhang and S. You, Synthesis of nitrogen and sulfur co-doped carbons with chemical blowing method for CO2 adsorption, *Fuel*, 2021, **305**, 121505.

26 J. Wei, D. Zhou, Z. Sun, Y. Deng, Y. Xia and D. Zhao,_A Controllable Synthesis of Rich Nitrogen-Doped Ordered Mesoporous Carbon for CO2 Capture and Supercapacitors, *Adv. Funct. Mater.*, 2013, **23**, 2322–2328.

27 S. C. Qi, X. J. Lu, Y. C. Lou, R. Zhou, D. M. Xue, X. Q. Liu and L. B. Sun,_Implementing an "Impracticable" Copolymerization to Fabricate a Desired Polymer Precursor for N-doped Porous Carbons, *Engineering*, 2022, **16**, 154–161.

28 H. Miao, W. Zhong, H. Yuan, W. Jiang and G. Hu, One-pot synthesis of nitrogen-doped carbons with hierarchically micro- and mesoporous structures for supercapacitors and CO2 capture, *New J. Chem.*, 2021, **45**, 6618–6629.

29 C. G. Wiener, Z. Qiang, Y. Xia, M. Tyagi and B. D. Vogt, Impact of surface wettability on dynamics of supercooled water confined in nitrogen-doped ordered mesoporous carbon, *Phys. Chem,. Chem. Phys.*, 2018, **20**, 28019–28025.

30 Z. Qiang, Y. Xia, X. Xia and B. D. Vogt, Generalized Synthesis of a Family of Highly Heteroatom-Doped Ordered Mesoporous Carbons. *Chem. Mat.*, 2017, **29**, 10178–10186.

31 Z. Qiang, Y. M. Chen, B. Gurkan, Y. Guo, M. Cakmak, K. A. Cavicchi, Y. Zhu and B. D. Vogt,_Cooperatively assembled, nitrogen-doped, ordered mesoporous carbon/iron oxide nanocomposites for low-cost, long cycle life sodium-ion batteries, *Carbon*, 2017, **116**, 286–293.

32 S.-C. Qi, D.-M. Xue, G.-X. Yu, R.-R. Zhu, X.-Q. Liu and L.-B. Sun, An antiempirical strategy: sacrificing aromatic moieties in the polymer precursor for improving the properties of the derived N-doped porous carbons *Green Chem. Eng.*, 2020, **1**, 70–76.

33 C. Ma, J. Bai, X. Hu, Z. Jiang and L. Wang,_Nitrogen-doped porous carbons from polyacrylonitrile fiber as effective CO2 adsorbents *J. Environ. Sci.*, 2023, **125**, 533–543.

34 J. Huang, J. Bai, M. Demir, X. Hu, Z. Jiang and L. Wang,_Efficient N-Doped Porous Carbonaceous CO2 Adsorbents Derived from Commercial Urea-Formaldehyde Resin *Energy Fuels*, 2022, **36**, 5825–5832.

35 S. C. Qi, Y. Liu, A. Z. Peng, D. M. Xue, X. Liu, X. Q. Liu and L. B. Sun, Fabrication of porous carbons from mesitylene for highly efficient CO2 capture: A rational choice improving the carbon loop, *Chem. Eng. J.*, 2019, **361**, 945–952.

36 C. Ma, J. Bai, M. Demir, X. Hu, S. Liu and L. Wang. Water chestnut shell-derived N/S-doped porous carbons and their applications in CO2 adsorption and supercapacitor, *Fuel*, 2022, **326**, 125119.

37 S. M. Hong, E. Jang, A. D. Dysart, V. G. Pol and K. B. Lee,_CO2 Capture in the Sustainable Wheat-Derived Activated Microporous Carbon Compartments, *Sci. Rep., 2016 6:1*, 2016, **6**, 1–10.

38 N. P. Wickramaratne and M. Jaroniec, *J. Mater. Chem. A.*, 2012, **1**, 112–116.

39 M. Sevilla, J. B. Parra and A. B. Fuertes, Importance of small micropores in CO2 capture by phenolic resin-based activated carbon spheres, *ACS Appl. Mater. Interfaces.*, 2013, **5**, 6360–6368.

40 M. M. Dubinin, Fundamentals of the theory of adsorption in micropores of carbon adsorbents: Characteristics of their adsorption properties and microporous structures, *Carbon*, 1989, **27**, 457–467.

41 J. Marszewska and M. Jaroniec, Tailoring porosity in carbon spheres for fast carbon dioxide adsorption, *J. Colloid Interface Sci.*, 2017, **487**, 162–174.

42 H. He, M. Zhong, D. Konkolewicz, K. Yacatto, T. Rappold, G. Sugar, N. E. David, J. Gelb, N. Kotwal, A. Merkle and K. Matyjaszewski, Three-Dimensionally Ordered Macroporous Polymeric Materials by Colloidal Crystal Templating for Reversible CO2 Capture, *Adv. Funct. Mater.*, 2013, **23**, 4720–4728.

43 L. Du, T. Lu and B. Li,_CO2 capture and sequestration in porous media with SiO2 aerogel nanoparticle-stabilized foams, *Fuel*, 2022, **324**, 124661.

44 F. Liu, K. Huang, C. J. Yoo, C. Okonkwo, D. J. Tao, C. W. Jones and S. Dai._Facilely synthesized meso-macroporous polymer as support of poly(ethyleneimine) for highly efficient and selective capture of CO2, *Chem. Eng. J.* 2017, **314**, 466–476.

45 S. Dutta, A. Bhaumik and K. C. W. Wu._Hierarchically porous carbon derived from polymers and biomass: effect of interconnected pores on energy applications, *Energy Environ. Sci.*, 2014, **7**, 3574–3592.

46 C. Chen, H. Huang, Y. Yu, J. Shi, C. He, R. Albilali and H. Pan, Template-free synthesis of hierarchical porous carbon with controlled morphology for CO2 efficient capture, *Chem. Eng. J*, 2018, **353**, 584–594.

47 Z. Zhang, Z. P. Cano, D. Luo, H. Dou, A. Yu and Z. Chen, Rational design of tailored porous carbon-based materials for CO2 capture, *J. Mater. Chem. A*. 2019, **7**, 20985–21003.

48 X. Q. Zhang, W. C. Li and A. H. Lu, Designed porous carbon materials for efficient CO2 adsorption and separation, *New Carbon Mater.*, 2015, **30**, 481–501.

49 J. M. Gu, W. S. Kim, Y. K. Hwang and S. Huh, Template-free synthesis of N-doped porous carbons and their gas sorption properties, *Carbon*, 2013, **56**, 208–217.

50 M. J. Behr, B. G. Landes, B. E. Barton, M. T. Bernius, G. F. Billovits, E. J. Hukkanen, J. T. Patton, W. Wang, C. Wood, D. T. Keane, J. E. Rix and S. J. Weigand, Structure-property model for polyethylene-derived carbon fiber, *Carbon*, 2016, **107**, 525–535.

51 M. A. Hunt, T. Saito, R. H. Brown, A. S. Kumbhar and A. K. Naskar, Pyrolysis pathways of sulfonated polyethylene, an alternative carbon fiber precursor, *Adv. Mater.*, 2012, **24**, 2386–2389.

52 P. J. Kim, H. D. Fontecha, K. Kim and V. G. Pol, Toward High-Performance Lithium-Sulfur Batteries: Upcycling of LDPE Plastic into Sulfonated Carbon Scaffold via Microwave-Promoted Sulfonation, *ACS Appl. Mater. Interfaces*, 2018, **10**, 14827–14834.

53 S. Villagómez-Salas, P. Manikandan, S. F. Acuña Guzmán and V. G. Pol, Amorphous Carbon Chips Li-Ion Battery Anodes Produced through Polyethylene Waste Upcycling, *ACS Omega*, 2018, **3**, 17520–17527.

54 M. Robertson, A. Güillen Obando, J. Emery and Z. Qiang, Multifunctional Carbon Fibers from Chemical Upcycling of Mask Waste, *ACS Omega*, 2022, **7**, 14, 12278-12287.

55 M. Robertson, A. G. Obando, B. Nunez, H. Chen and Z. Qiang, Upcycling Mask Waste to Carbon Capture Sorbents: A Combined Experimental and Computational Study, *ACS Appl. Eng. Mater.,* DOI:10.1021/ACSAENM.2C00030.

56 P. Maji and K. Naskar, Styrenic block copolymer-based thermoplastic elastomers in smart applications: Advances in synthesis, microstructure, and structure‐property relationships—A review, *J. Appl. Polym. Sci.*, 2022, **139**, e52942.

57 G. Lee, M. Eui Lee, S. S. Kim, H. I. Joh and S. Lee, Efficient upcycling of polypropylene-based waste disposable masks into hard carbons for anodes in sodium ion batteries, *J. Ind. Eng. Chem.*, 2022, **105**, 268–277.

58 X. Hu and Z. Lin, Transforming waste polypropylene face masks into S-doped porous carbon as the cathode electrode for supercapacitors, *Ionics*, 2021, **27**, 2169–2179.

59 J. E. Coughlin, A. Reisch, M. Z. Markarian and J. B. Schlenoff, Sulfonation of polystyrene: Toward the "ideal" polyelectrolyte, *J. Polym. Sci. A. Polym. Chem.*, 2013, **51**, 2416–2424.

60 K. W. Kim, H. M. Lee, J. H. An, B. S. Kim, B. G. Min, S. J. Kang, K. H. An and Y. J. Kim, Effects of cross-linking methods for polyethylene-based carbon fibers: review, *Carbon Lett.*, 2015, **16**, 147–170.

61 J. M. Younker, T. Saito, M. A. Hunt, A. K. Naskar and A. Beste,_Pyrolysis pathways of sulfonated polyethylene, an alternative carbon fiber precursor, *J. Am. Chem. Soc.*, 2013, **135**, 6130–6141.

62 E. S. Zofchak, J. A. Lanasa, W. Mei and R. J. Hickey,_Polymerization-Induced Nanostructural Transitions Driven by In Situ Polymer Grafting, 2018, **7**, 822–827.

63 R. Zhang, Z. Qiang and M. Wang,_Integration of Polymer Synthesis and Self-Assembly for Controlled Periodicity and Photonic Properties, *Adv. Funct. Mater.*, 2021, **31**, 2005819.

64 Z. Qiang, S. A. Akolawala and M. Wang,_Simultaneous In-Film Polymer Synthesis and Self-Assembly for Hierarchical Nanopatterns, *ACS Macro Lett.*, 2018, **7**, 566–571.

65 X. Li, Q. Xue, X. Chang, L. Zhu, C. Ling and H. Zheng,_Effects of Sulfur Doping and Humidity on CO2 Capture by Graphite Split Pore: A Theoretical Study, *ACS Appl. Mater. Interfaces*, 2017, **9**, 8336–8343.

66 S. Feng, W. Li, Q. Shi, Y. Li, J. Chen, Y. Ling, A. M. Asiri and D. Zhao,_Synthesis of nitrogen-doped hollow carbon nanospheres for CO2 capture, *Chem. Comm.*, 2013, **50**, 329–331.

67 Á. Sánchez-Sánchez, F. Suárez-García, A. Martínez-Alonso and J. M. D. Tascón,_Influence of porous texture and surface chemistry on the CO2 adsorption capacity of porous carbons: Acidic and basic site interactions, *ACS Appl. Mater. Interfaces*, 2014, **6**, 21237–21247.

68 Y. Sun, J. Zhao, J. Wang, N. Tang, R. Zhao, D. Zhang, T. Guan and K. Li,_Sulfur-Doped Millimeter-Sized Microporous Activated Carbon Spheres Derived from Sulfonated Poly(styrene-divinylbenzene) for CO2 Capture, *J. Phys. Chem. C*, 2017, **121**, 10000–10009.

69 D. Saha, G. Orkoulas, J. Chen and D. K. Hensley,_Adsorptive separation of CO2 in sulfur-doped nanoporous carbons: Selectivity and breakthrough simulation, *Microporous Mesoporous Mater.*, 2017, **241**, 226–237.

70 J. Wang and S. Kaskel,_KOH activation of carbon-based materials for energy storage, *J. Mater. Chem.*, 2012, **22**, 23710–23725.

71 Y. Lv, F. Zhang, Y. Dou, Y. Zhai, J. Wang, H. Liu, Y. Xia, B. Tu and D. Zhao,_A comprehensive study on KOH activation of ordered mesoporous carbons and their supercapacitor application, *J. Mater. Chem.*, 2011, **22**, 93–99.

72 S. Shingdilwar, D. Kumar, B. Sahu and S. Banerjee,_Straightforward synthesis of multifunctional porous polymer nanomaterials for CO 2 capture and removal of contaminants, *Polym. Chem.*, 2022, **13**, 2165–2172.

73 S. Shingdilwar, S. Dolui and S. Banerjee,_Facile Fabrication of Functional Mesoporous Polymer Nanospheres for CO2 Capture, *Ind. Eng. Chem. Res.*, 2022, **61**, 1140–1147.

74 M. G. Mohamed, W.-C. Chang and S.-W. Kuo,_Crown Ether- and Benzoxazine-Linked Porous Organic Polymers Displaying Enhanced Metal Ion and CO2 Capture through Solid-State Chemical Transformation, *Macromolecules*, DOI:10.1021/ACS.MACROMOL.2C01216.

75 C. Xu, C. Q. Ruan, Y. Li, J. Lindh and M. Strømme. High-Performance Activated Carbons Synthesized from Nanocellulose for CO2 Capture and Extremely Selective Removal of Volatile Organic Compounds, *Adv. Sustain Syst*, 2018, **2**, 1700147.

76 D. Li, J. Zhou, Z. Zhang, L. Li, Y. Tian, Y. Lu, Y. Qiao, J. Li and L. Wen._Improving low-pressure CO2 capture performance of N-doped active carbons by adjusting flow rate of protective gas during alkali activation, *Carbon*, 2017, **114**, 496–503.

.